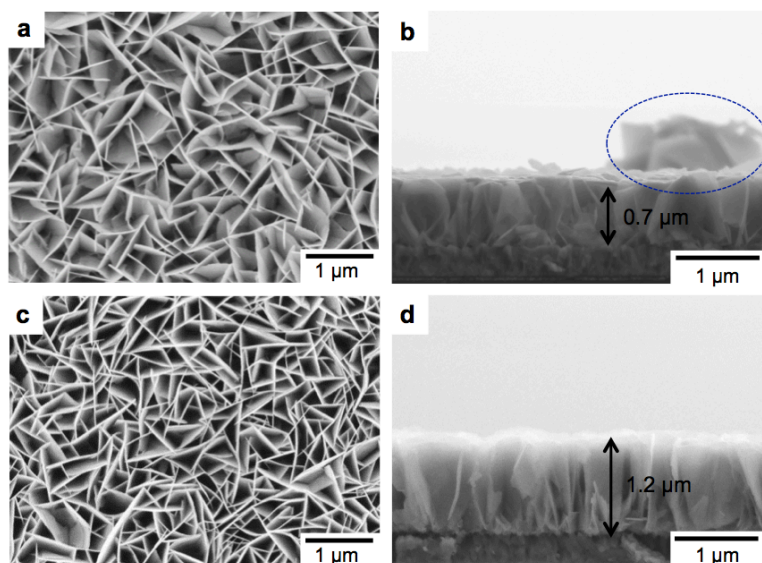


In the format provided by the authors and unedited.

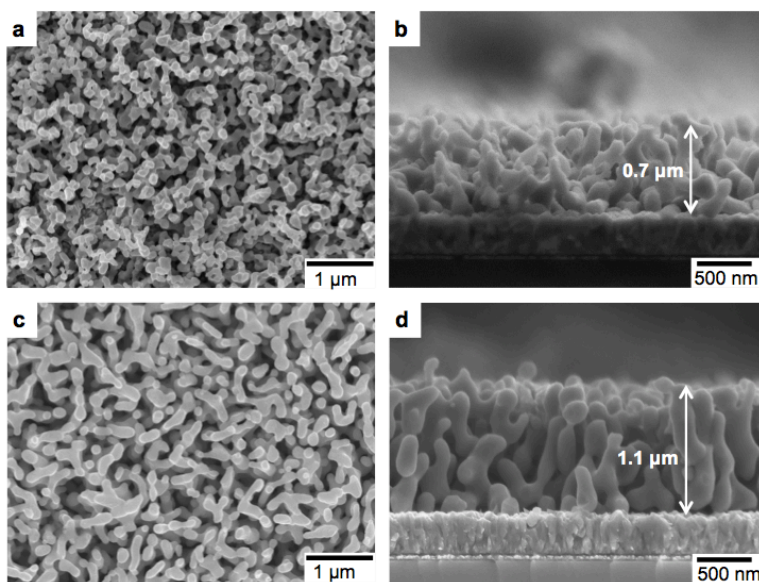
Enhancing long-term photostability of BiVO₄ photoanodes for solar water splitting by tuning electrolyte composition

Dong Ki Lee  and Kyoung-Shin Choi *

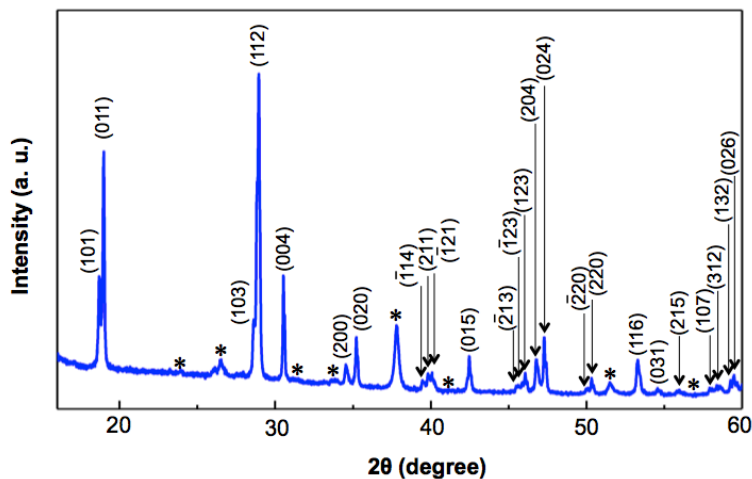
Department of Chemistry, University of Wisconsin-Madison, Madison, WI, USA. *e-mail: kschoi@chem.wisc.edu



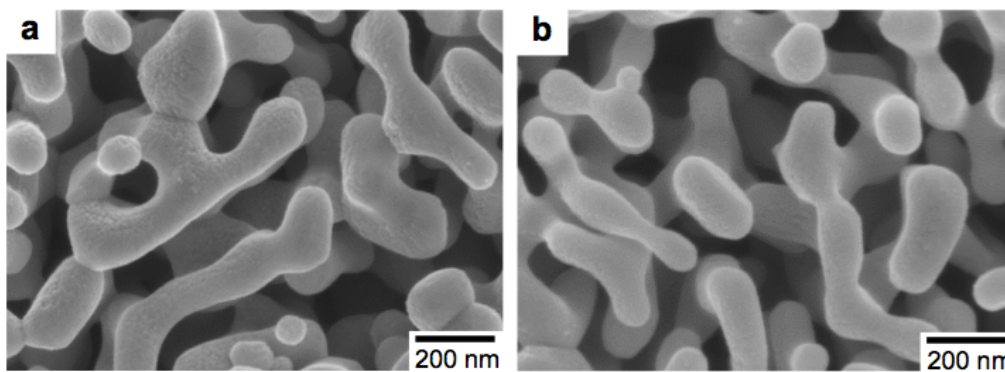
Supplementary Figure 1. Comparison of SEM images of BiOI electrodes deposited using (a-b) the previously reported conditions and (c-d) the modified conditions of the current study. The comparison of the top-view images (a,c) clearly shows the effect of a newly added nucleation step, increasing the nucleation density of BiOI crystals. The modified conditions passed almost three times more charge but, due to the significantly enhanced nucleation density, the increase in the film thickness was only 71% as shown in (b,d). The use of the lactate buffer and a more dilute Bi^{3+} and *p*-benzoquinone solution also ensured a more uniform growth of the film. For example, the additional nucleation of BiOI on top of the initial layer of BiOI crystals, marked with a dotted circle in (c), is suppressed in (d).



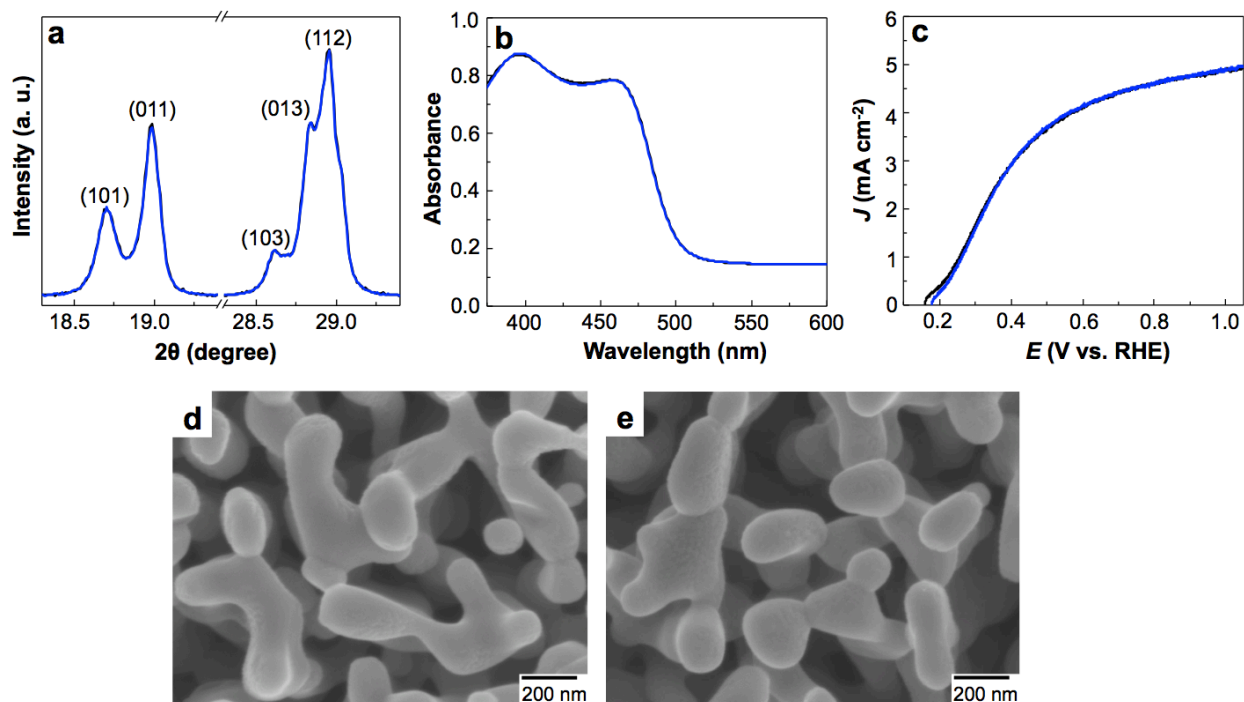
Supplementary Figure 2. Comparison of SEM images of BiVO_4 electrodes prepared using (a-b) the previously reported conditions and (c-d) the modified conditions of the current study.



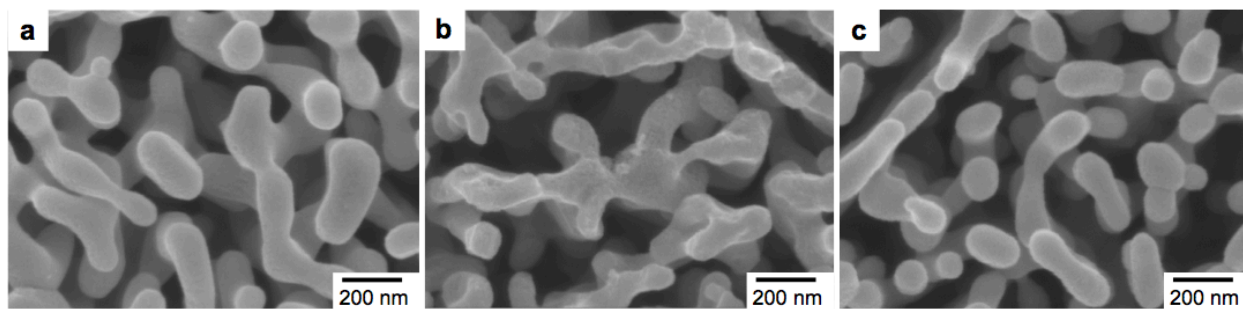
Supplementary Figure 3. XRD pattern of the N₂-treated BiVO₄ electrode used in this study showing the high crystallinity and purity of BiVO₄ (JCPDS 83-1699). Asterisks represent peaks from the FTO substrate.



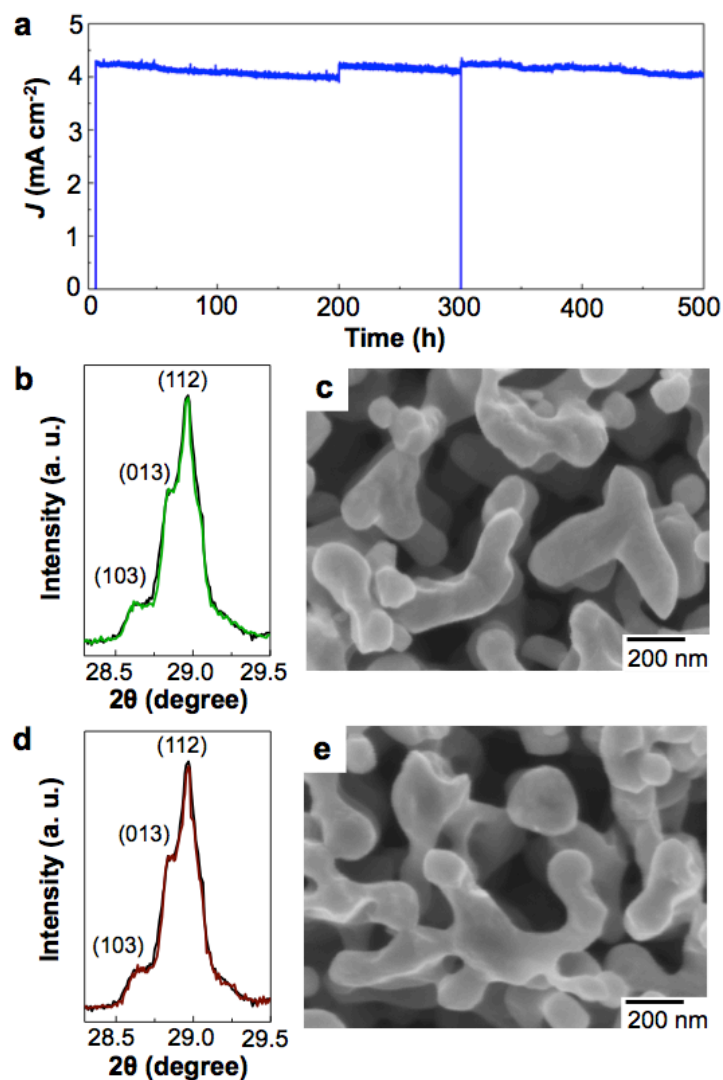
Supplementary Figure 4. High magnification SEM images of BiVO₄ (a) before and (b) after the deposition of FeOOH/NiOOH OEC layers. Since the OEC layers were extremely thin, no noticeable morphology change was observed except that the surface became slightly smoother.



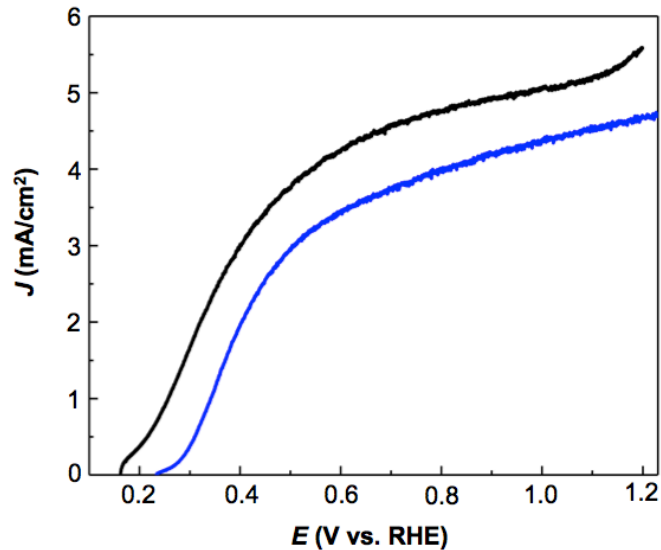
Supplementary Figure 5. (a) XRD patterns, (b) UV-vis spectra, and (c) photocurrent measurements for sulfite oxidation of BiVO_4 before (black) and after (blue) immersion in KB (pH 9.3) for 50 days. SEM images of (d) before and (e) after immersion are also shown. No changes are shown in these results confirming the chemical stability of our BiVO_4 electrodes in a pH 9 solution. J-V plots for sulfite oxidation were measured in KB (pH 9.3) containing 0.2 M Na_2SO_3 (AM 1.5G, 100 mW/cm^2 illumination, scanning rate of 10 mV/s).



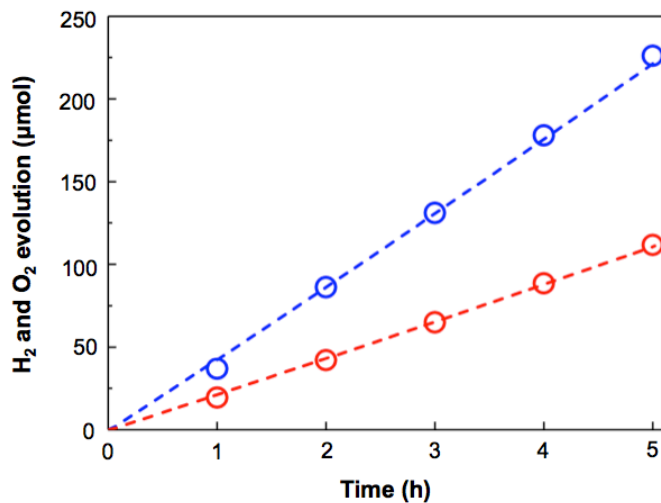
Supplementary Figure 6. SEM images of $\text{BiVO}_4/\text{FeOOH}/\text{NiOOH}$ (a) before and (b) after J-t measurement at 0.6 V vs. RHE in KB solution for 60 h. The dissolution of BiVO_4 is evident in (b). (c) SEM image of $\text{BiVO}_4/\text{FeOOH}/\text{NiOOH}$ after J-t measurement at 0.6 V vs. RHE for 60 h in KB+V solution. No change in morphology is observed when comparing (a) and (c).



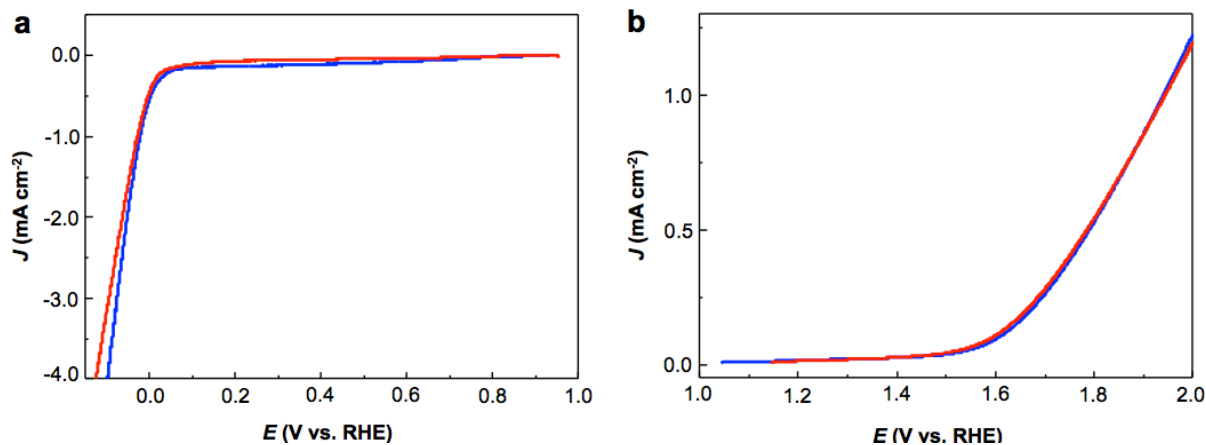
Supplementary Figure 7. (a) J - t plot of BiVO₄ for sulfite oxidation at 0.6 V vs. RHE in 0.5 M KB solution (pH 9.3) containing 0.7 M Na₂SO₃. The slight photocurrent decrease observed over time is not due to photocorrosion but due to the depletion of sulfite. When the solution was replaced with a fresh sulfite solution, the photocurrent returned back to its initial value. XRD and SEM image of the BiVO₄ at (b-c) 300 h and (d-e) 500 h. XRD of the original film is shown in black in (b) and (d), which perfectly match with the green (300 h) and brown (500 h) lines, indicating no loss of mass or crystallinity.



Supplementary Figure 8. J-V plots of BiVO_4 for sulfite oxidation (black) in the KB solution containing 0.2 M Na_2SO_3 (pH 9.3) and $\text{BiVO}_4/\text{FeOOH}/\text{NiOOH}$ for water oxidation (blue) in the KB solution (pH 9.3) (AM 1.5G, $100 \text{ mW}/\text{cm}^2$ illumination, scanning rate of 10 mV/s).



Supplementary Figure 9. Detection of H_2 (blue circle) and O_2 (red circle) gases produced by the $\text{BiVO}_4/\text{FeOOH}/\text{NiOOH}$ at 0.6 V vs. RHE in the KB+V solution. The dotted lines represent theoretical amounts of H_2 and O_2 assuming 100% Faradaic efficiency.



Supplementary Figure 10. Linear sweep voltammograms obtained using a Pt electrode as the WE in KB (blue) and KB+V (red) solutions; (a) from the open circuit potential to the negative direction and (b) from the open circuit potential to the positive direction. These results show that the presence of V⁵⁺ in the KB+V solution does not produce any additional reduction or oxidation peaks and does not interfere with water reduction or water oxidation.

Supplementary Table 1. Differences between the previously reported [13, 14] and current conditions for BiOI deposition.

	Plating Solution			Deposition Condition	
	Bi(NO ₃) ₃ (mM)	<i>p</i> -benzoquinone (mM)	lactic acid (mM)	applied potential (V vs. Ag/AgCl)	charge passed (C/cm ²)
Previous	40	230	-	-0.10	0.13
Current	15	46	30	-0.35 → -0.10	0.37

Supplementary Table 2. Differences between the deposition conditions for the FeOOH/NiOOH dual-layer OECs used in the previous [13, 14] and current studies.

	Plating Solution		Charge Passed (mC/cm ²)		Atomic Fe:Ni ratio in the OEC layer
	FeOOH	NiOOH	FeOOH	NiOOH	
Previous	100 mM FeSO ₄	100 mM NiSO ₄	67.5	21.0	8:2
Current	5 mM FeSO ₄ + 100 mM K ₂ SO ₄	Pre-soaking:50 mM NiSO ₄ Deposition:100 mM K ₂ SO ₄	8.3	4.2 (2.1×2)	9:1

Supplementary Table 3. EDS data of FeOOH/NiOOH electrodes before and after 60 h J-t measurement in KB, KB+V, and KB+Fe+Ni solutions.

Atomic concentration (at.%)	After J-t for 60 h			
	Before J-t	KB	KB+V	KB+Fe+Ni
Fe	2.70	2.82	3.37	2.93
Ni	0.32	0.36	0.56	0.38
V	0.00	0.00	0.63	0.00
O	57.93	57.28	55.92	57.07
Sn (from FTO)	30.90	30.75	31.01	30.82
Relative ratio to Sn (%)				
Fe/Sn	8.74	9.17	10.87	9.51
Ni/Sn	1.04	1.17	1.81	1.23
V/Sn			2.03	